Journal of Advanced Research in Fluid Mechanics and Thermal Sciences

Journal homepage:
https://semarakilmu.com.my/journals/index.php/fluid_mechanics_thermal_sciences/index
ISSN: 2289-7879

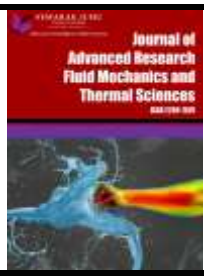

Simulation of Torque, Tip Speed Ratio, Power, and Power Coefficient of 1 MW Horizontal Axis Wind Turbine in Modified NACA 4412-2412 Variation of Airfoil Blades

Kriswanto[1,*], Mohammad Misbachul Munir[1], Dony Hidayat Al-Janan[1], Samsudin Anis[1], Rizqi Fitri Naryanto[1], Arimaz Hangga[1], Wirawan Sumbodo[1], Rusiyanto[1], Andri Setiyawan[1], Aldias Bahatmaka[1], Imam Sukoco[1], Basyirun[1], Naufal Baihaqi Al Afkar[2], Jamari Jamari[3]

[1] Department of Mechanical Engineering, Universitas Negeri Semarang, Gd E5 Kampus UNNES, Semarang, Indonesia
[2] School of Mechanical Engineering, University of Adelaide, North Terrace, South Australia, 5005, Australia
[3] Department of Mechanical Engineering, University of Diponegoro, Jl. Prof. Sudharto Kampus UNDIP, Semarang, Indonesia

ARTICLE INFO

Article history:
Received 23 April 2024
Received in revised form 30 July 2024
Accepted 13 August 2024
Available online 30 August 2024

Keywords:
Airfoil; blade element momentum; HAWT; leading edge; airfoil modification; trailing edge

ABSTRACT

The rotor power of HAWT can be affected by the type of airfoil and airfoil modifications on a blade. However, no study of wind turbine blades from arranges types of airfoils or altering the leading and trailing edges has been conducted. To determine the maximum torque, TSR, power, and power coefficient values at Horizontal Axis Wind Turbine (HAWT) 1MW, simulations of turbine blades with various airfoil designs are performed. NACA 4412 and 2412 airfoils were utilized, with the leading and trailing edges modified. The method used is Blade Element Momentum simulation on 20 blade variations with modified NACA airfoils. The HAWT simulation parameters use the specifications of a 1MW wind turbine with a blade radius of 54m, wind speed of 7 m/s, number of blades 3. Due to the aerodynamic simulation results, the percentage error between the CFD from the other study and the BEM values is only 2.6%. The blade code that produces high torque on the HAWT is 4T-4LT (4412 TE mod-4412 LE-TE mod). The high torque value is influenced by the lift and drag coefficients. High torque does not usually imply high power; rather, the TSR as a function of angular speed determines this. The angular speed of a horizontal axis wind turbine is visibly affected by the aerodynamics of the rotor blade. C4412-2412 group combination blade designs, particularly blade codes 4L-2LT, 4T-2LT, 4LT-2L, 4LT-2T, and 4LT-2LT, can produce more than 1MW. The highest TSR, power, and coefficient power of HAWT was obtained from blades with circular foil segments 1 and 2, segments 3 to 9 using NACA 4412 LE-TE mod airfoil, and segments 10 to 11 using NACA 2412 LE-TE airfoil. Although the difference is slight (0.20%), the combination of modified trailing and leading edge NACA 4412 and 2412 airfoils outperforms modified leading edge airfoils alone.

* *Corresponding author.*
E-mail address: kriswanto@mail.unnes.ac.id

https://doi.org/10.37934/arfmts.120.2.155173

1. Introduction

The renewable energy development that has high potential is wind energy because of its easy utilization, high stability, and cost-effectiveness [1]. Due to its abundant and non-polluting nature, wind energy is considered to have great potential and can increase quickly for electricity production compared to other renewable energies [2]. Wind turbines have potential for use in Southeast Asia; one such country is Indonesia, where wind speeds can reach 4 to 7 m/s [3]. The wind speed is categorized as low-medium on the basis of the Beaufort scale [4]. Additionally, although the medium wind speed classification has the potential to be used, it hasn't yet been able to provide highly efficient power. For small-capacity power plants with a 10–100 kW capacity, wind speeds of 7 m/s are often adequate [5]. Therefore, it is required to design a wind turbine blade that generates maximum power. The rotor is the main part that influences the performance of the Horizontal Axis Wind Turbine (HAWT) because it is designed to capture as much wind energy as possible to convert it into electrical power. The power efficiency of wind turbines depends on the aerodynamic characteristics of the rotor blades being designed [6]. HAWT has been developed into various variations based on the number of blades because turbine efficiency is be affected by the number of blades applied to the turbine rotor [7].

Typically, the design of the rotor HAWT affects the power produced, as well as the parts and considerations that go into constructing a suitable blade. The airfoil type and attack angle are variables that must be taken into consideration in the HAWT's blade development [8]. According to research, the most effective rotor design used 55xx blades to create a power of around 500 kW at 9 m/s wind speed (0020, 0018, 0015, 0012, 5520, 5518, 5515, and 5512) [9]. The maximum lift coefficient is found when the angle of attack increases, according to a BEM analysis of the best attack angle for the NACA 0012 and NACA 2412 blades. Furthermore, the NACA 2412 airfoil outperforms the NACA 0012 in terms of maximum power and efficiency at a tip speed ratio of 7 [10].

The NACA 2412 airfoil exhibits higher efficiency at a tip speed ratio (TSR) of 7 then produces a maximum power output in comparison to the NACA 0012 airfoil, according to research on the best angle of attack for the NACA 0012 and NACA 2412 blades to obtain the maximum lift and drag ratio using the BEM [11]. The effect of adjusting the pitch angle with variations in displacement, specifically +6°, +3°, 0°, -3°, and -6°, to obtain the power coefficient for TSR variations from 3 to 7 using BEM calculations, as well as the fact that the pitch angle setting of 0° and +3° has the best influence on turbine efficiency [12]. The SD7080 airfoil was analyzed to have the optimum lift coefficient value and lift-to-drag ratio in a study optimization of small-scale wind turbine design on the variants of NASA airfoils [13].

Blade Element Momentum (BEM) can be used to design and analyze horizontal axis wind turbines in addition to using CFD solutions. QBlade is software based on BEM theory and has been used extensively for simulation, optimization, and validation of HAWT designs [14]. Much research has been carried out on changes to standard airfoil designs to get maximum power HAWT. In comparing the standard NASA LS (1)-0413 airfoil with a similar airfoil modified at the leading edge, the result was that the airfoil experienced an increase in performance of 27.8% [15]. Analysis of the trailing edge modification of the NACA 4412 and NACA 2412 airfoils on a 1 MW HAWT yields the lift coefficient value increased by 0.002 on both modified airfoils compared to the standard airfoil. Changes in the two airfoils affect the HAWT rotor power [16].

Optimization of a 1 MW wind turbine with variations in airfoil, angle of attack, and pitch angle using the Taguchi method and ANOVA analysis found that the most significant parameter affecting turbine power was the type of airfoil with a contribution value of 42.34%. Furthermore, the angle of attack has a contribution value of 32.16%, and the most contribution is the pitch angle (17.09%) [8].

Blade design and optimization using the CFD method on the NACA 4412, NACA 0012, NACA 4418, and NACA 0015 airfoil variations has been carried out and obtained the best Cl value on the NACA 4412 of 1.13154 [17]. Analysis and optimization of the HAWT aerodynamic characteristics with airfoil SG-604 derived the highest C_p value was 0.35 [18]. The optimization and selection of airfoil blades in small-scale wind turbines shows that the type of airfoil on the turbine blade influences the power coefficient and turbine startup time [19].

HAWT power simulation using the QBlade program on changes in wind speed affecting HAWT rotor power obtained that the higher the wind speed, the more ideal the power value. A higher power coefficient value results in more wind energy, which, depending on the TSR value, can be converted into mechanical energy [20]. When compared to wind turbines without additional bumps, airfoil leading edge modification for wind turbine rotors resulted in a greater lift coefficient [21]. Airfoil analysis with the inclusion of bumps on the wings of aircraft to improve operating performance at a specific angle of attack [22-24].

Based on the previous study above, the type of airfoil and airfoil modifications on the wind turbine blade can affect power. However, there has been no analysis of wind turbine blades from combining types of airfoils or modifying the leading and trailing edges to obtain optimal turbine power above 1 MW. Simulations of the turbine blades with various airfoil configurations are carried out to know the maximum torque, TSR, power, and power coefficient values at HAWT 1MW. The airfoil as a shape of the HAWT blade influences the aerodynamic characteristics and performance. This research aims to determine the torque, TSR, power, and power coefficient values of a 1 MW HAWT from blade variations with a combination of modified NACA 4412 and NACA 2412 airfoils on the leading edge and trailing edge at low wind speeds (7 m/s).

2. Methodology

This study uses blade element momentum simulation with software to determine maximum torque, TSR, power, and power coefficient. BEM theory combines two methods, namely the blade element method and momentum theory. The blade element method tests the force produced by the lift and drag coefficients of the airfoil. Momentum theory is the balance of momentum of the air rotating through the turbine [25].

Based on BEM theory, the blade is divided into several elements, where each part has a certain twist angle and chord length [19]. BEM theory is widely used due to its simple operation and appropriate calculation accuracy [26]. Another advantage is that BEM theory requires more time and cost efficiency when compared to other popular methods, for example, Computational Fluid Dynamics (CFD) [27].

The blade is divided into numerous segments, with the assumption that each element is independent and that the fluid flow is unidirectional. The force and moment of each segment must be computed. As a result, the total of forces and moments was an integration of each element's forces and moments [28,29]. Thrust is generated on each blade segment based on blade element theory, as shown in Eq. (1). Therefore, the torque acting on each segment can be calculated using Eq. (1) based on Figure 1 [8].

$$dT = B\frac{1}{2}\rho V_{total}^2(C_l \cos\varphi + C_d \sin\varphi)\, cdr \tag{1}$$

Following the determination of thrust, the torque acting on each blade segment can be computed using the equation

$$dQ = B\frac{1}{2}\rho V_{total}^2 \left(C_l \sin\varphi - C_d \cos\varphi\right) crdr \tag{2}$$

$$V_{total} = \sqrt{{U_\infty}^2 + (\omega r)^2} \tag{3}$$

where dT is the thrust, dQ is the torque on the blade sections, B is the number of blades, ρ is the air density, V_{total} is the resulting velocity, C_l is the lift coefficient, ω is the blade rotation speed, C_d is the drag coefficient, φ is the inflow angle, c is the airfoil chord, and r is the element radius from the hub.

$$dT = 4\pi r\rho U_\infty^2 \left(1 - a\right) adr \tag{4}$$

$$dQ = 4\pi r^3 \rho U_\infty \Omega (1 - a)\, a' dr \tag{5}$$

$$a' = \frac{\omega}{2\Omega} \tag{6}$$

where U_∞ is the natural wind speed, Ω is the angular speed, and a' = axial induction factor. The force acting on an airfoil is the angle of attack (α), and the chord line to the line of rotation is the pitch angle (β), as shown in Figure 1(a) and Figure 1(b) [8].

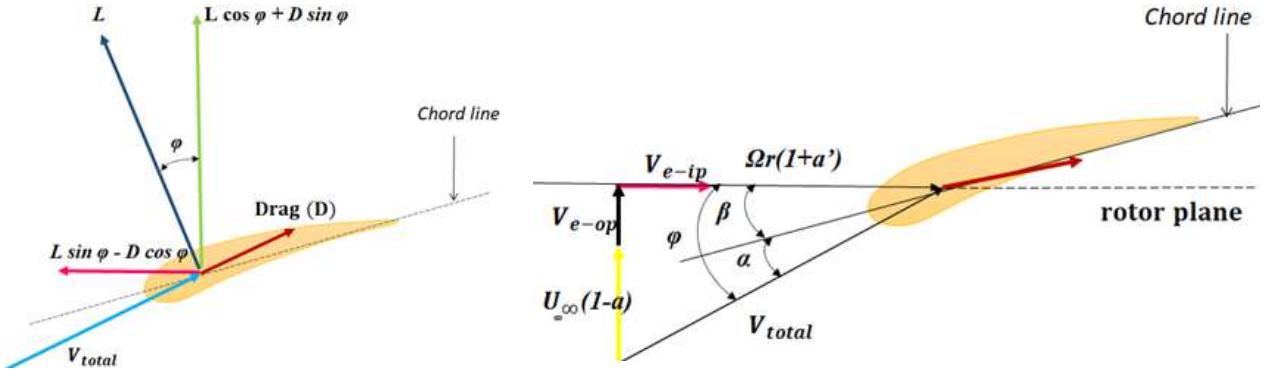

(a) (b)

Fig. 1. Local element (a) forces (b) velocities and flow angles [8]

The angle of attack, as shown in Figure 2, is known as the angle between the relative wind speed line at the leading edge and the chord line. The magnitude of the lifting and drag forces varies depending on variations of the angle of attack. A large lift will occur when the angle of attack is small, while the drag force is small when the angle of attack is certain. The twist and pitch of the blade are affected by the angle of attack [30].

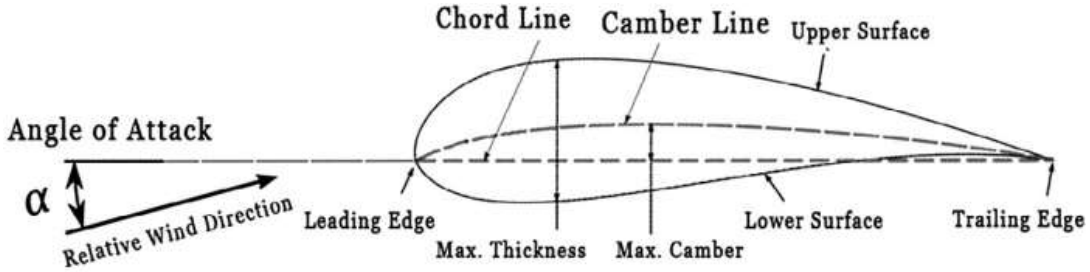

Fig. 2. Angle of attack [30]

Rotor power is the mechanical power produced by the turbine rotor. Torque is the rotational force resulting from the rotation of the turbine shaft. Rotor power and torque calculated by the equation

$$P_{rotor} = \tau\omega \tag{7}$$

$$\tau = Fl \tag{8}$$

where P_{rotor} is the power rotor (W), τ is the torque (Nm), and ω is the the angular velocity (rad/s), F is the force (N), and l is the turbine blade length (m).

The power coefficient is the ratio of the power generated by the rotor to the available wind energy. Based on the Betz limit theory, wind turbines cannot convert all the energy from the wind. Therefore, theoretically, the optimum C_p value that can be achieved by wind turbines is 0.593 [31]. The equation is used to determine the power coefficient.

$$C_p = \frac{P_{rotor}}{P_{wind}} \tag{9}$$

where C_p is the power coefficient, P_{rotor} is the rotor power (W), and P_{wind} is the wind power (W).

TSR is the ratio between the tip speed of the rotor blades and the wind speed. The TSR, λ equation is as follows

$$\lambda = \frac{\omega r}{U_\infty} \tag{10}$$

where λ is the Tip Speed Ratio, U_∞ is the wind speed (m/s)*, and r* is the rotor radius (m).

The BEM simulation uses QBlade to determine the torque, TSR, C_p, and power values of a 1 MW HAWT. The HAWT parameters used are as in Table 1. Table 1 presents the HAWT parameters in this study and refers to previous research [8]. Apart from that, the HAWT with a diameter of 54 m is still below the size of the commercial HAWT made by Siemens Gamesa type SG 2.1-114 with a diameter of 56 m [32]. These commercial HAWTs have been installed in many countries and on various continents.

The HAWT rotor design consists of 3 blades with a blade length of 54 meters devided into 11 segments. Furthermore, segments 1 and 2 use a circular foil, while the next segment uses a combination of two modified airfoils. In segments 3 to 9 uses a modified airfoil of the first variation, and segments 10 and 11 use a different modified airfoil from the previous segment. An illustration of the blade design is shown in Figure 3. Segment position size (Position), Chord Length (L_c), and the shape (airfoils) of each segment are presented in Table 2.

Table 1
The 1 MW HAWT parameters [8]

Specification	Value
Blades number	3
Wind speed, *v* (m/s)	7
Air density, *ρ* (kg/m^3)	1.225
Length of blade, *l* (m)	54
Radius of hub, r_1 (m)	1.25
Tower height, *h* (m)	110
Swept Area, *A* (m^2)	10,023.67

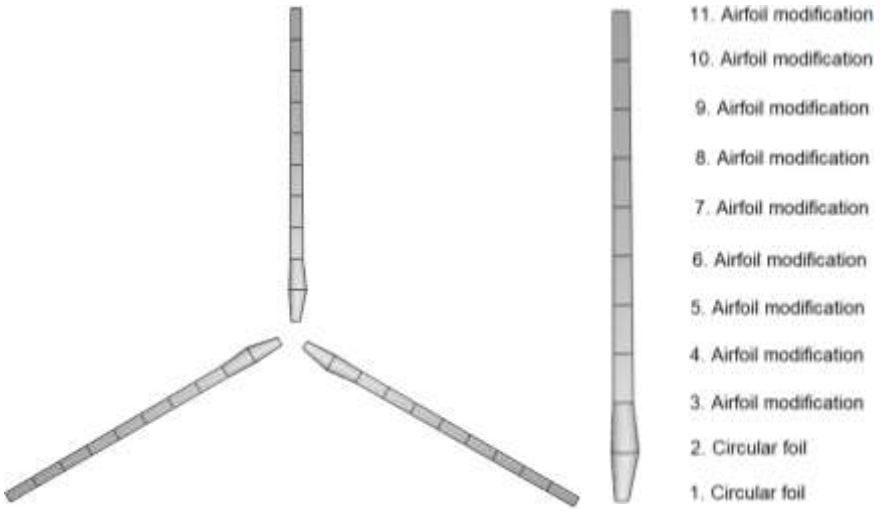

Fig. 3. Rotor design of the 1 MW HAWT model

Table 2
Shape and dimension blade segment

Segment	Segment position, L_{pos} (m)	Chord length, L_c (m)	Shape
1	0	1.5	Circular foil
2	5.4	3	Circular foil
3	10.8	2.2	Airfoil modification
4	16.2	2.15	Airfoil modification
5	21.6	2.1	Airfoil modification
6	27	2.05	Airfoil modification
7	32.4	2	Airfoil modification
8	37.8	1.95	Airfoil modification
9	43.2	1.9	Airfoil modification
10	48.6	1.85	Airfoil modification
11	54	1.8	Airfoil modification

As shown in Table 3, this study used six modified airfoils from Airfoil NACA 4412 and NACA 2412. Modifications were made to the leading edge (LE), trailing edge (TE), and leading-trailing edge (LE-TE) on both NACA airfoils.

Table 3
Type of airfoil for each segment in blade variations

No	Blade Code	Shape of blade segment		
		Segment 1-2	Segment 3-9	Segment 10-11
1	4L-4LT	Circular foil	4412 LE mod	4412 Mod LE-TE
2	4LT-4L	Circular foil	4412 LE-TE mod	4412 LE mod
3	4T-4LT	Circular foil	4412 TE mod	4412 LE-TE mod
4	4LT-4T	Circular foil	4412 LE-TE mod	4412 Mod TE
5	4LT	Circular foil	4412 LE-TE mod	4412 LE-TE mod
6	2L-2LT	Circular foil	2412 LE mod	2412 LE-TE mod
7	2LT-2L	Circular foil	2412 LE-TE mod	2412 LE mod
8	2T-2LT	Circular foil	2412 TE mod	2412 LE-TE mod
9	2LT-2T	Circular foil	2412 LE-TE mod	2412 TE mod
10	2LT	Circular foil	2412 LE-TE mod	2412 LE-TE mod
11	4L-2LT	Circular foil	4412 LE mod	2412 LE-TE mod
12	4T-2LT	Circular foil	4412 TE mod	2412 LE-TE mod
13	4LT-2L	Circular foil	4412 LE-TE mod	2412 LE mod
14	4LT-2T	Circular foil	4412 LE-TE mod	2412 TE mod
15	4LT-2LT	Circular foil	4412 LE-TE mod	2412 LE-TE mod
16	2L-4LT	Circular foil	2412 LE mod	4412 LE-TE mod
17	2T-4LT	Circular foil	2412 TE mod	4412 LE-TE mod
18	2LT-4L	Circular foil	2412 LE-TE mod	4412 LE mod
19	2LT-4T	Circular foil	2412 LE-TE mod	4412 TE mod
20	2LT-4LT	Circular foil	2412 LE-TE mod	4412 LE-TE mod

The NACA 4412 Airfoil design was modified from its standard shape. The NACA 4412 LE mod airfoil (Figure 4) has 11 leading edge points of the NACA 4412 airfoil on chord points 0 m to 0.176 m, which are modified and changed to 11 points from the NACA 2410 airfoil so that the modified airfoil has a higher lift coefficient [8]. NACA 4412 TE mod airfoil (Figure 5) has 6 points on the trailing edge of the NACA 4412 airfoil at chord points 1.98 m to 2.2 m, which are modified so that the airfoil has a higher lift coefficient than the standard NACA 4412 [16]. The NACA 4412 LE-TE mod airfoil (Figure 6) is the combination of the NACA 4412 LE mod airfoil and the NACA 4412 TE mod so that the shape changes are on the leading edge (LE) and trailing edge (TE). The change in shape of the NACA 4412 airfoil before and after the modification is calculated by the difference in an area using Eq. (10). The area difference of the airfoil after modification is less than 0.2%, as shown in Table 4.

$$\text{Change of areas, } \Delta_A \text{ (\%)} = \frac{A_0 - A_{mod}}{A_0} \times 100\% \quad (11)$$

where A_0 is the area of NACA airfoil standard, A_{mod} is the area of NACA modification airfoils.

Table 4
Difference in NACA 4412 airfoil area before and after modification

Airfoil	Area, A_{foil} (m^2)	Change of areas, Δ_A (%)
NACA 4412	0.397896	
NACA 4412 LE mod	0.397603	0.07
NACA 4412 TE mod	0.397735	0.04
NACA 4412 LE-TE mod	0.397425	0.12

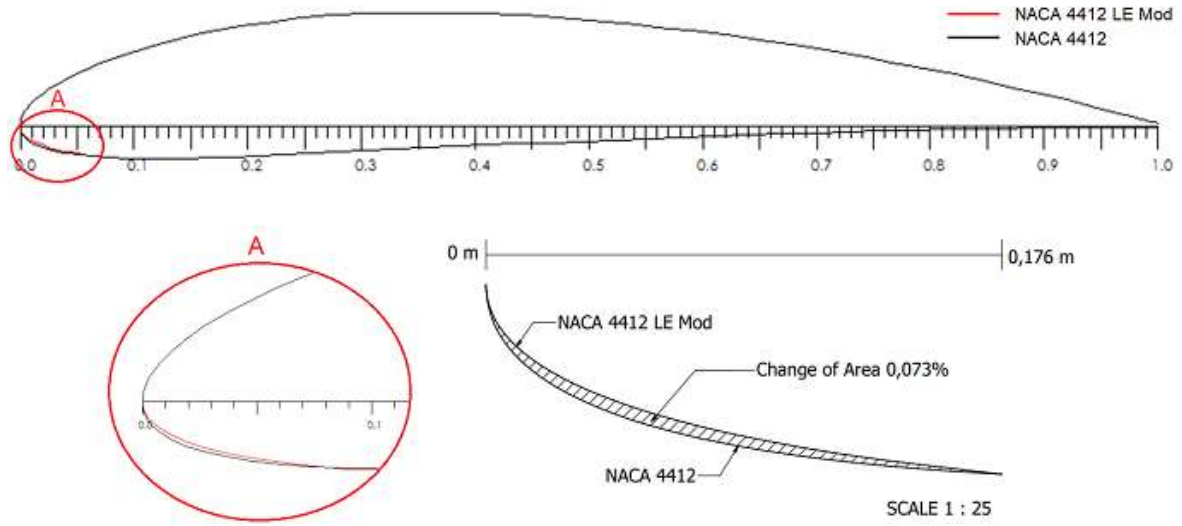

Fig. 4. Geometry of NACA 4412 LE mod airfoil

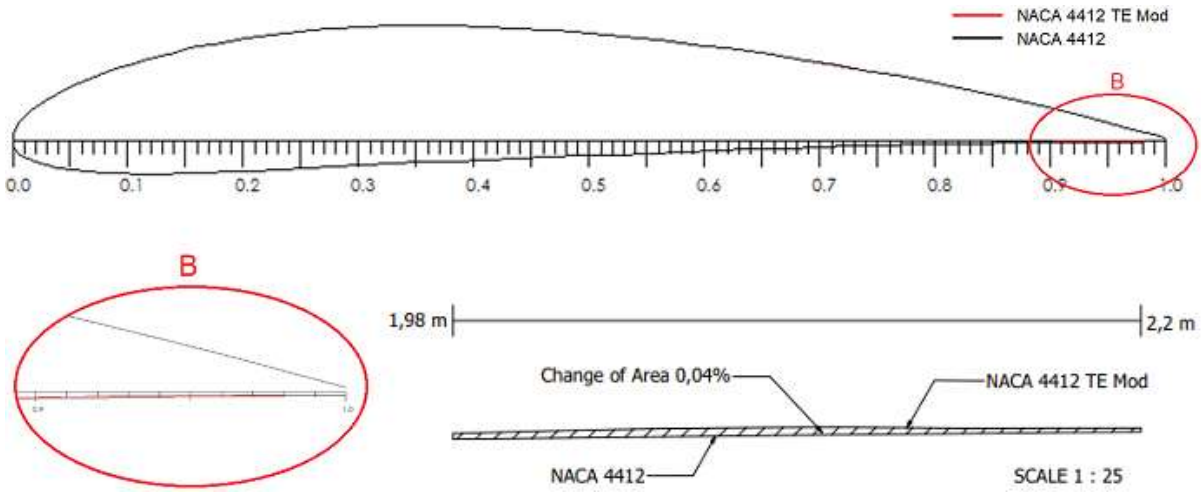

Fig. 5. Geometry of NACA 4412 TE mod airfoil

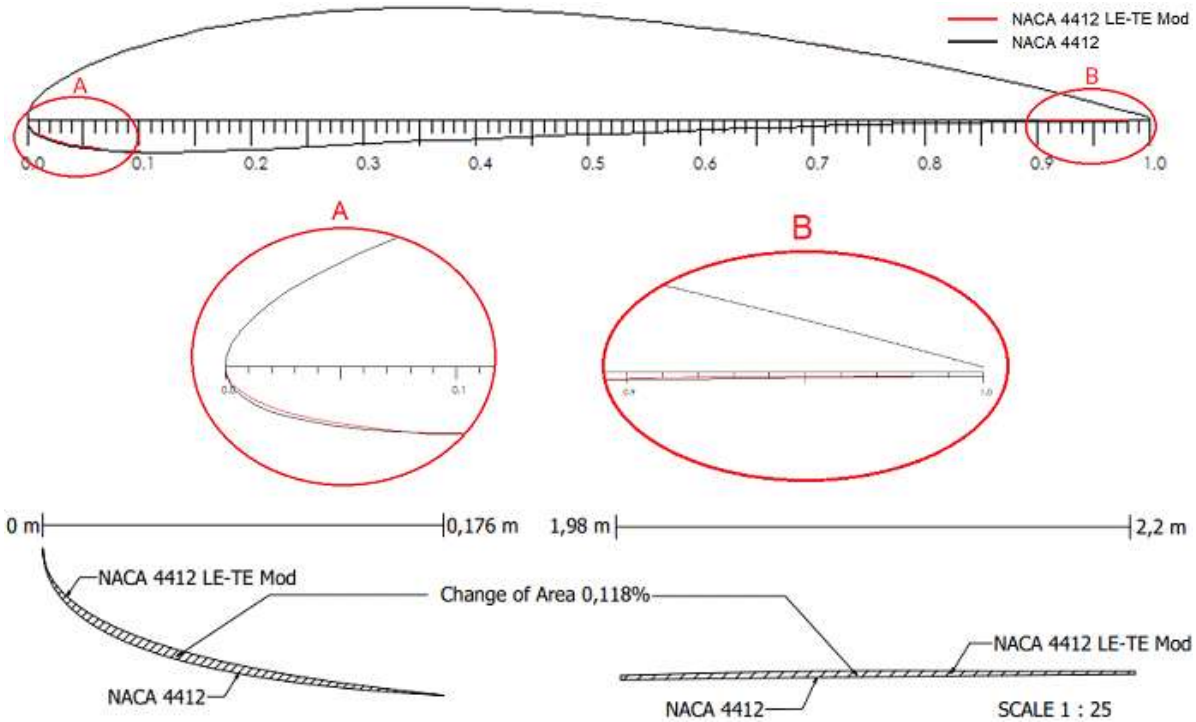

Fig. 6. Geometry of NACA 4412 LE-TE mod airfoil

The NACA 2412 LE mod airfoil (Figure 7) has 11 leading edge points of the NACA 2412 airfoil at chord points 0 m to 0.026 m that changed with 11 points from the NACA 1410 airfoil so that the modified airfoil has a higher lift coefficient [8].

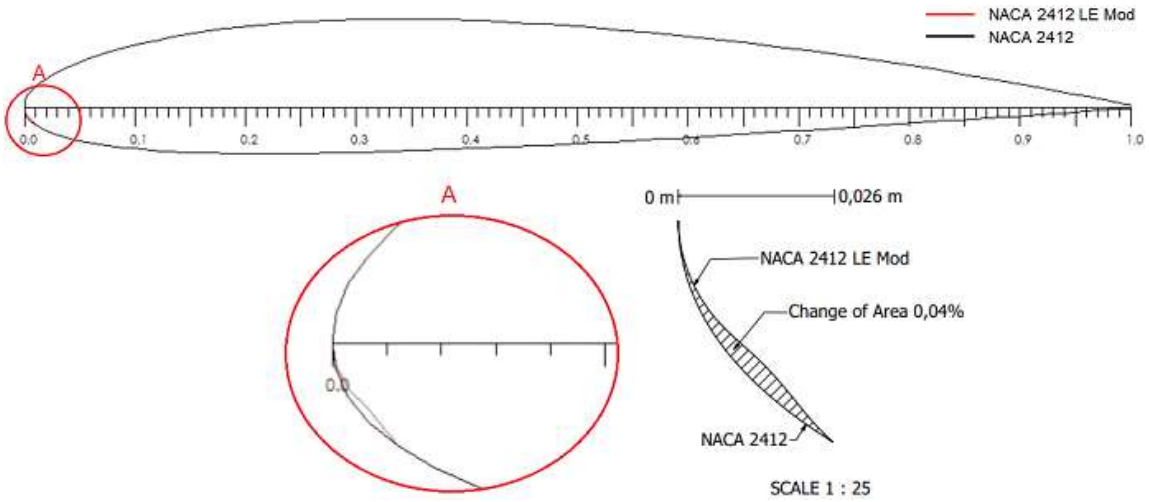

Fig. 7. Geometry of NACA 2412 LE mod airfoil

NACA 2412 TE mod airfoil (Figure 8) has 6 points on the trailing edge at chord points 1.98 m to 2.2 m that was modified, so the airfoil has a higher lift coefficient than the standard NACA 2412 [16]. The NACA 2412 LE-TE mod (Figure 9) combines the NACA 2412 LE mod airfoil and the NACA 2412 TE mod, similar with the NACA 4412 LE-TE mod. The airfoil changes are found on the leading edge (LE) and trailing edge (TE). The difference area of the airfoil after modification is less than 0.2%, as shown in Table 5.

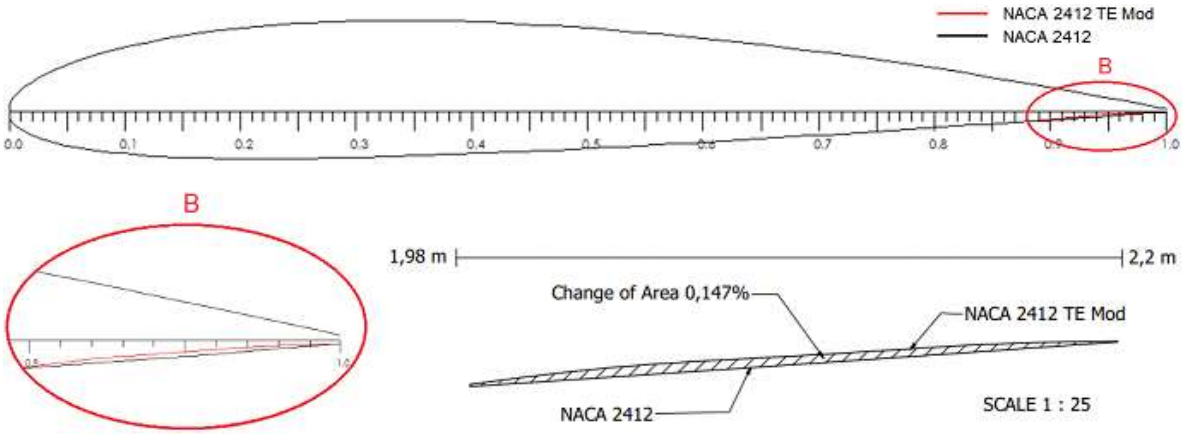

Fig. 8. Geometry of NACA 2412 TE mod airfoil

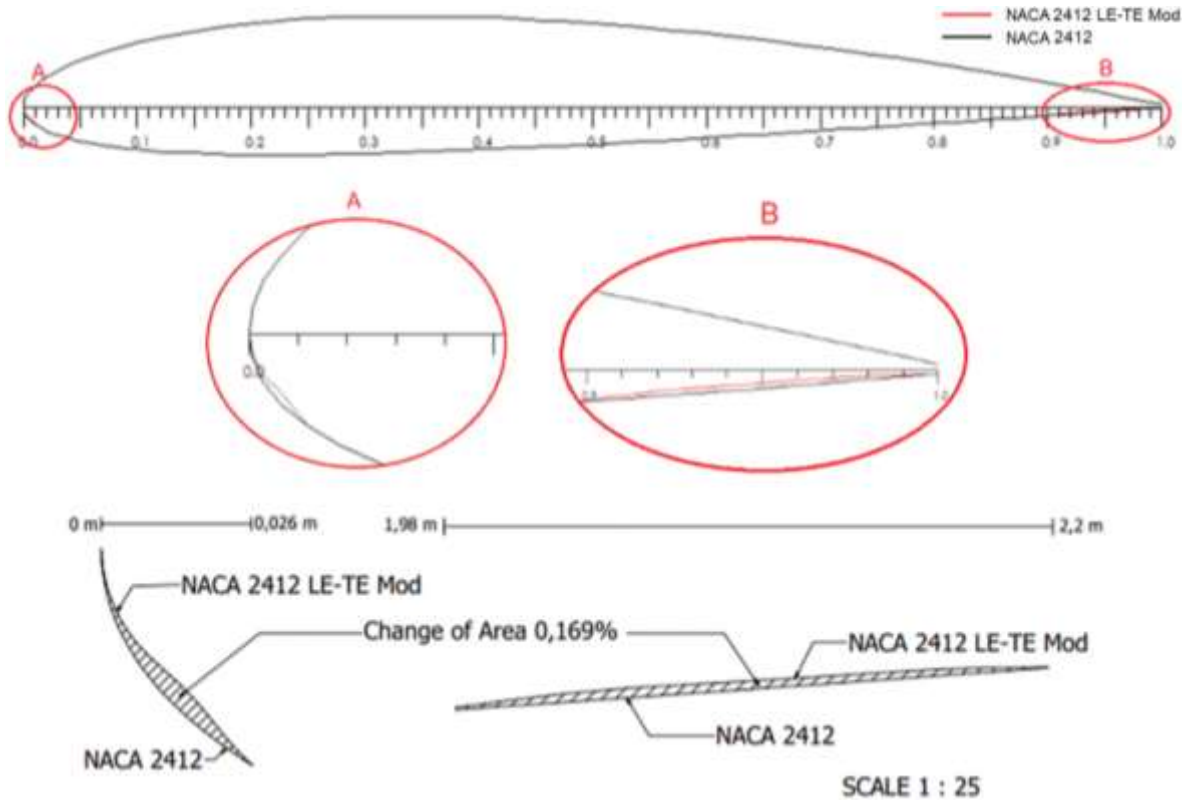

Fig. 9. Geometry of NACA 2412 LE-TE mod airfoil

Table 5
Difference in NACA 2412 airfoil area before and after modification

Airfoil	Area, A_{foil} (m^2)	Change of areas, Δ_A (%)
NACA 2412	0.397971	
NACA 2412 LE mod	0.397809	0.04
NACA 2412 TE mod	0.397385	0.15
NACA 2412 LE-TE mod	0.397298	0.12

3. Results

This study uses a validation test to confirm the validity level of the results with prior studies that used the Computational Fluid Dynamics (CFD). The study of the rotor using CFD with the parameters presented in Table 6 shows that the CFD simulation in research by Yin *et al.,* [33] produces a power

of 255 Watt with these parameters. Rotor power simulation using BEM base to the parameters Table 6 obtained a rotor power of 262 Watts, as shown in Figure 10.

$$\% \, error = \frac{X_1 - X_0}{X_1} \times 100\% \tag{12}$$

where X_1 is the rotor power in present study, and X_0 is the rotor power from CFD.

Table 6
Differences of power rotor HAWT of CFD method vs. BEM simulation (present study)

Parameters	Simulation Model	
	CFD	BEM
Airfoil	NACA 4412	NACA 4412
Blades number	3	3
Wind speed, *v* (m/s)	11.5	11.5
Length of blade, *l* (m)	0.575	0.575
Power, *P* (W)	255	262
% Error	2.6%	

The aerodynamic simulation results show that the percentage error between the CFD from study by Yin *et al.,* [33] and the BEM values is only 2.6%. As a result, the desired conditions are followed by the BEM aerodynamic simulation on the HAWT rotor. Validation was also acquired by reviewing research by Koç *et al.,* [34] that compared the CFD and the BEM using the rotor parameters listed in Table 6. Validation between the two models, CFD and BEM, is undertaken to guarantee that the turbine performance values are realistic [35]. The computational domain mesh has a considerable impact on CFD simulation accuracy [36]. This method also serves as a model for analyzing wind turbine performance using mechanical, geometric, and feature aspects [37]. The advantages of the BEM model are that it is less expensive and takes less time to compute than the CFD model [38-43].

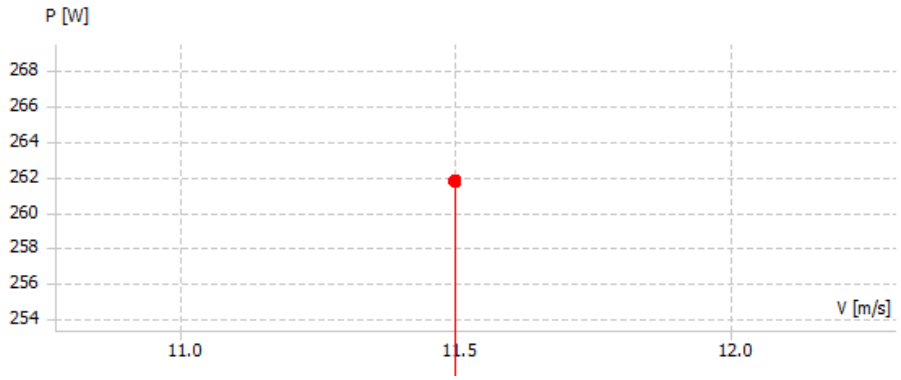

Fig. 10. HAWT power rotor using BEM simulation

The selection of the angle of attack is carried out by simulating the power and power coefficients using the BEM software. The blade uses the NACA 4412 LE mod – 4412 LE-TE mod airfoil configuration wherein the HAWT parameter settings follow Table 1. The angle of attack is varied from 0-25° with a discrete 5°. The simulation results (Table 7) show that the highest power value (997,325 W) and the highest power coefficient (0.473) are found in blades with an angle of attack of 0°. Furthermore, the angle of attack 0° was used as a fixed parameter in this simulation.

Based on Table 7, the highest power and power coefficient results are at an angle of attack of 0°, while the lowest is at an angle of attack of 25°. As the blade's angle of attack increases, the power and power coefficient decrease. Another study by Kriswanto *et al.,* [16], the HAWT power simulation

on the NACA 4412 and 2412 airfoil modifications, revealed a loss in power as the angle of attack rose. The greater the angle of attack, the more airflow passing through the airfoil cannot flow until it touches the airfoil rear, which causes air turbulence at the airfoil rear. As a result, the lifting force on the HAWT blade is not optimal, resulting in decreased wind turbine performance [44].

Table 7
Rotor power simulation results based on variations in attack angle

Attack angle, α (°)	Torque, τ (Nm)	TSR	Power, *P* (W)	C_p
0°	1,141,760	8.02	997,325	0.473
5°	1,167,940	6.94	949,366	0.451
10°	978,626	6.58	798,114	0.379
15°	548,927	7.9	537,094	0.255
20°	367,871	7.42	338,150	0.160
25°	103,897	8.25	105,081	0.050

Airfoil selection is an important factor in designing horizontal axis wind turbines. The configuration of the wind turbine airfoil also affects the power generated. The blade design on a horizontal axis wind turbine uses thicker airfoils at the base (near the hub) to withstand bending moments and structural pressures, while smaller/thinner airfoils on the primary/tip/blade ends produce more aerodynamic torque so that kinetic energy can be maximum conversion [45].

The airfoil on the blade should be divided into three sections: the root, primary, and tip for the root part. While the root section has to support all of the aerodynamic, gravitational, centrifugal, gyroscopic, and operational loads operating on the blade, structural aspects are more significant than aerodynamic. As a result, the cross-section of the turbine blade's root portion is thick. Thin airfoils are utilized as the primary and tip sections to reduce drag. Aerodynamics takes precedence over structural factors in this case. In this part, the lift force rotates the blades, which drives the generator to generate energy [25].

The standard and modified NACA 4412 airfoils were simulated to determine the lift and drag coefficient value, and the magnitude of the difference was calculated using the Eq. (12) and Eq. (13). The lift and drag coefficient difference between the modified and standard of the NACA airfoils is present in Table 8 and Figure 11.

$$\%\ diff\ Cl = \frac{C_{ls} - C_{la,b,c}}{C_{ls}} \times 100\% \tag{13}$$

$$\%\ diff\ Cd = \frac{C_{ds} - C_{da,b,c}}{C_{ds}} \times 100\% \tag{14}$$

where C_{ls} is the lift coefficient of NACA 4412 airfoil standard, $C_{l\,a,b,c}$ is the lift coefficient of NACA 4412 modification airfoils, C_{ds} is the drag coefficient of NACA 4412 airfoil standard, $C_{d\ a,b,c}$ is the drag coefficient of NACA 4412 modification airfoils.

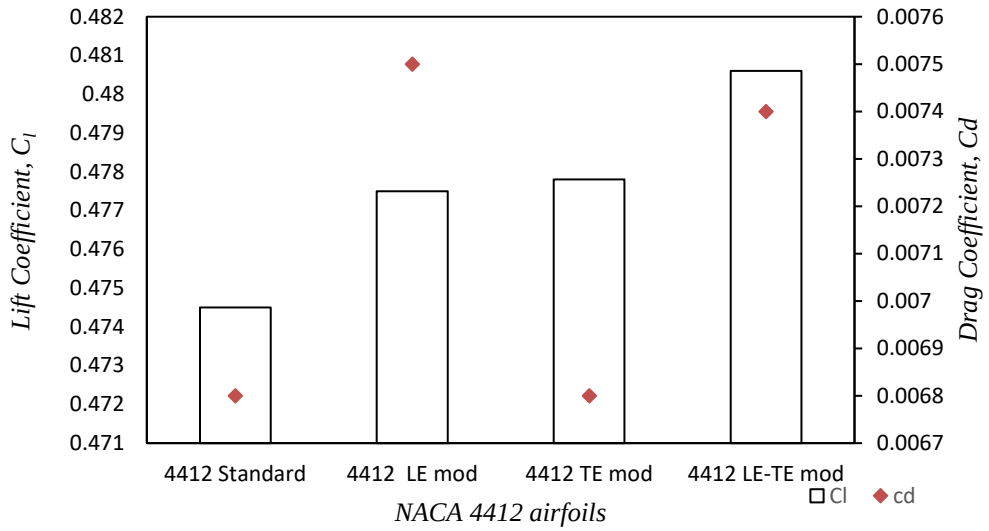

Fig. 11. NACA 4412 standard and modified Lift and drag coefficient values

Table 8
The lift and drag coefficient of NACA 4412 standard and modifications

Airfoils	C_l	Difference C_l (%)	C_d	Difference C_d (%)
4412 Standard	0.4745	-	0.0068	-
4412 LE mod	0.4775	0.62	0.0075	10.29
4412 TE mod	0.4778	0.69	0.0068	0
4412 LE-TE mod	0.4806	1.27	0.0074	8.82

Standard and modified NACA 2412 airfoils were also simulated to obtain lift coefficient values, and differences were calculated using the Eq. (12). The percentage of C_l difference between the airfoils shows that the blade with the 2412 LE-TE mod airfoil compared to the standard has a high percentage difference, namely 1.27% (Table 9). The NACA 4412 standard lift and drag coefficient values and modifications are in Figure 12.

NACA 4412 leading edge modified (4412 LE mod) airfoils have the highest drag coefficient of 10.29 (Figure 11) compared to modified or standard NACA 4412. The C_d value on the NACA 2412 leading edge mod is the same as the NACA 2412 trailing edges, which is 0.0075. The percentage difference in C_d between standard NACA 2412 and modified NACA on the leading edge is 41.07%. The modified Naca 4412 trailing edge gets a lower C_d value than the standard NACA 2412, with a difference of 1.78%.

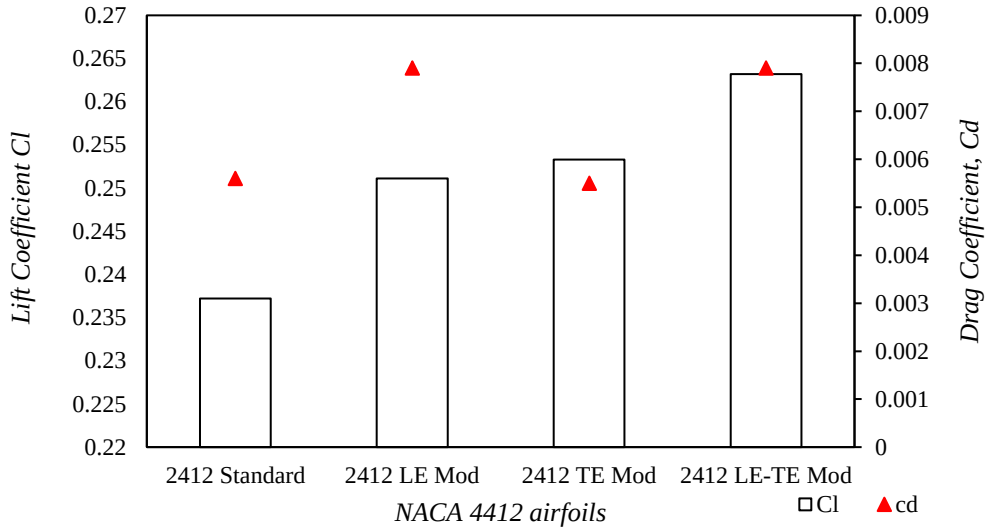

Fig. 12. NACA 2412 standard and modified coefficient lift values

Table 9
The lift coefficient of NACA 2412 standard and modification

Airfoils	C_l	Difference C_l (%)	C_d	Difference C_d (%)
2412 Standard	0.2372		0.0056	
2412 LE mod	0.2511	5.53	0.0079	41.07
2412 TE mod	0.2533	6.35	0.0055	-1.78
2412 LE-TE mod	0.2633	9.87	0.0079	41.07

Simulation of HAWT blade airfoil modification variations through BEM software QBlade obtains torque, tip speed ratio, power, and power coefficient results, shown in Table 10.

Table 10
Turbine simulation results based on various types of modified airfoils

No	Blade Code	Combination grup	Torque, τ (Nm)	TSR	Power, *P* (W)	*Cp*
1	4L-4LT	A4412-4412	1,004,100	8.02	997,325	0.4734
2	4LT-4L		971,915	8.25	994,141	0.4718
3	4T-4LT		1,004,830	8.01	998,046	0.4737
4	4LT-4T		970,934	8.26	993,138	0.4714
5	4LT		970,921	8.25	993,125	0.4711
6	2L-2LT	B2412-2412	817,205	8.86	896,402	0.4255
7	2LT-2L		816,970	8.85	896,145	0.4253
8	2T-2LT		817,084	8.84	896,270	0.4254
9	2LT-2T		817,073	8.85	896,258	0.4254
10	2LT		817,065	8.85	896,250	0.4253
11	4L-2LT	C4412-2412	927,466	8.85	1,017,350	0.4829
12	4T-2LT		927,722	8.86	1,017,631	0.4830
13	4LT-2L		927,457	8.85	1,017,340	0.4829
14	4LT-2T		927,560	8.85	1,017,453	0.4829
15	4LT-2LT		927,835	8.87	1,017,754	0.4831
16	2L-4LT	D2412-4412	903,744	7.77	870,878	0.4133
17	2T-4LT		905,474	7.78	872,545	0.4141
18	2LT-4L		905,063	7.78	872,149	0.4139
19	2LT-4T		905,039	7.78	872,125	0.4139
20	2LT-4LT		905,347	7.78	872,422	0.4141

The highest torque on the 4T-4LT blade code (1,004,830 Nm), while the lowest is the 2LT-2LT blade code (817,065Nm), as shown in Figure 13. The torque difference between blades is close, where the A4412-4412 combination is 3.37%, the B2412-2412 combination is 0.028%, the C4412–2412 combination is 0.04%, and the D2412–4412 combination is 0.19%. Furthermore, the torque value of the 2412-2412 combination is the lowest because the lift coefficient value is the lowest and the drag coefficient is the highest compared to the others.

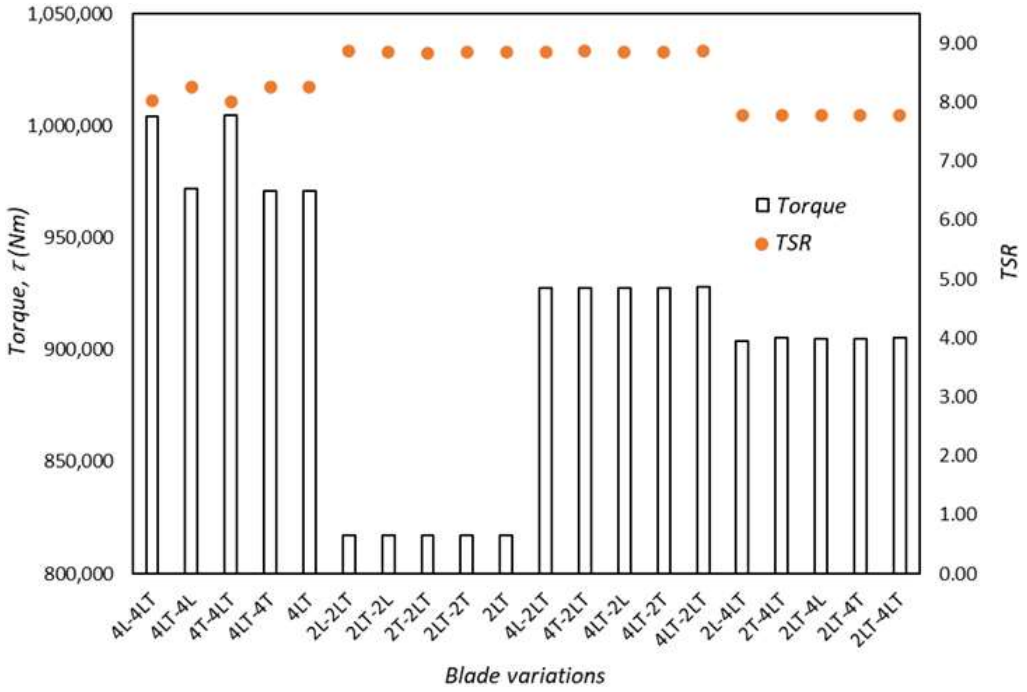

Fig. 13. Blade variations vs torque and TSR

A fascinating fact regarding the contributing factors is the coexistence of almost identical blades and marginally varied torque values [46]. The torque on the 4T-4LT blade (1,004,830Nm) is higher than the 4L-4LT (1,004,100Nm) this is because the C_l value of code 4412 TE (0.4778) is higher than C_l 4412 LE (0.4775) and the C_d value of 4412TE (0.0068) is lower than C_d 4412 LE (0.0068). At the same entering velocity, the lift and drag coefficients of Table 11 compares the values between the two modified blades where the high C_d value on the 4412 LE causes calculation results with a low inflow angle, which reduces the torque value.

Table 11
Blade, airfoil, lift and drag coefficient, and inflow angle at segment 3 (pos=10.8m); φ = 16.52°

No	Blade	Airfoil	C_l	C_d	$C_l \sin\varphi - C_d \cos\varphi$
1	4L-4LT	4412 LE mod	0,4775	0,0075	0,1286
2	4T-4LT	4412 TE mod	0,4778	0,0068	0,1293

Blade code 4T-4LT consists of segments 3 to 9 using NACA 4412 TE mod with C_l of 0.4775 and C_d of 0.0068 then segments 10 to 11 using NACA 4412 LE-TE with C_l of 0.4806 and C_d of 0.0074.

The highest TSR value (8.87) is for blade code 4LT-2LT, while the lowest (7.77) is for blade code 2L-4LT. The TSR difference between blades is close, where the A4412-4412 combination is 3.02%, the B2412-2412 combination is 0.22%, the C4412-2412 combination is 0.22%, and the D2412-4412 combination is 0.13%. TSR affects how quick the wind turbine rotates. The higher the TSR, the higher the angular velocity, which increases the power and power coefficient of the wind turbine. The 4LT-

2LT blade code has the highest TSR (8.87), resulting in the highest HAWT power (1,017,754) and the highest power coefficient (0.4831). Simulation results using blade element momentum (BEM) in Figure 14 for power and power coefficient values according to theoretical Eq. (6) and Eq. (9).

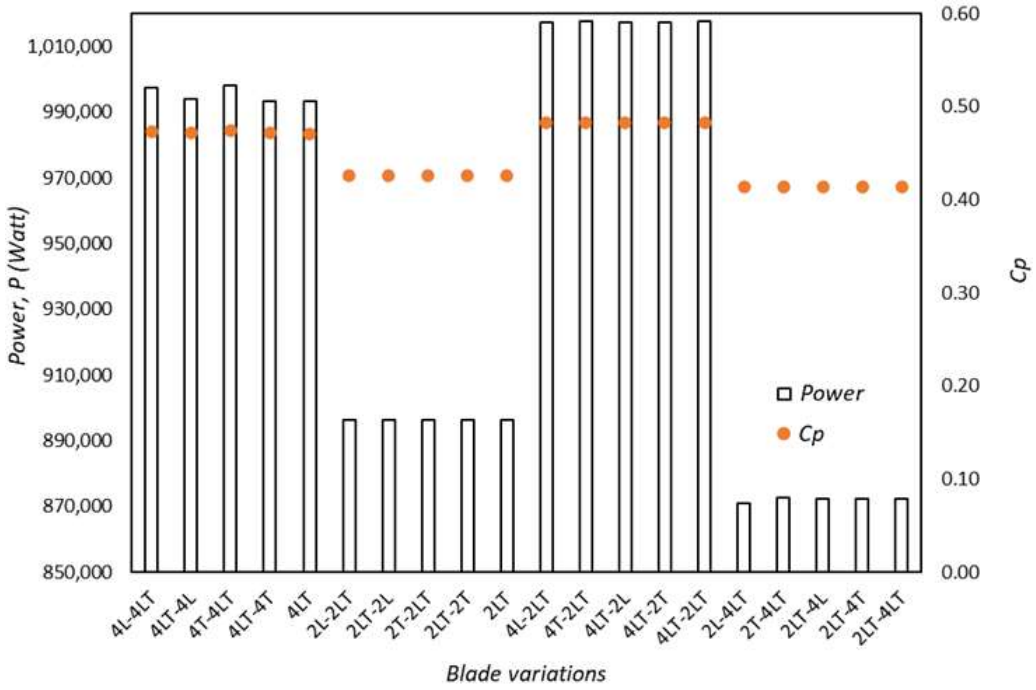

Fig. 14. Blade variations vs power and power coefficient

Similar previous research on optimizing HAWT rotor power with variations in wind speed, airfoil, and angle of attack obtained the highest rotor power on blades with NACA 4412 and 2412 airfoils modified at the trailing edge point [16]. The lift coefficient is increased by 0.69 for NACA 4412 and 6.53 for NACA 2412 airfoils are modified compared to the standard. The rotor power at 7m/s wind speed is 1.037 MW, which is more than the power of the current study (1.018 MW) because the present research blade's variation in radius size is 1 meter smaller. The torque value affects the turbine power value, while the blade radius affects the torque value.

Other studies modified the leading edge of NACA 4412 and NACA 2412 airfoils, which raised the lift coefficient compared to the standard but was less significant than alterations to the trailing edge [8,16]. The results of HAWT IMW rotor power optimization with variations in airfoil, angle of attack, and pitch angle obtained a power of 1,016 MW on the leading edge modified NACA 4412 and NACA 2412 airfoil at an angle of attack of 0° and a pitch angle of 0°. The most significant parameter analysis that influences turbine power is the airfoil.

The blade variations that can produce above 1MW are blade designs C4412-2412 group combination, namely blade codes 4L-2LT, 4T-2LT, 4LT-2L, 4LT-2T, and 4LT-2LT. The modified airfoil affects the lift and torque coefficients and influences the angular speed value of the turbine blade. The higher TSR value in this simulation (Table 10) increases the HAWT power value. The high TSR is due to the high rotational speed resulting from the influence of the airfoil profile of each segment. The highest HAWT power (1,017,754 W) was obtained from blades with circular foil segments 1 and 2, segments 3 to 9 using NACA 4412 LE-TE mod airfoil, and segments 10 to 11 using NACA 2412 LE-TE airfoil.

This study's HAWT rotor power is more than that of the comparable research by Kriswanto *et al.,* [16] with identical parameters, proving the superiority of the modified NACA 4412 and 2412 at the leading edge and trailing edge.

4. Conclusions

The difference between the CFD from the other study and the BEM (present study) is only 2.6%, BEM method is valid and use in this study. Furthermore, the variation angle of attack (0;5;10;15;20) was simulated using BEM and obtained that an angle of attack of 0° produced maximum power and then used in parameter setup. The NACA 4412 and NACA 2412 airfoils with the leading and trailing edges modified have the highest lift coefficient compared to other modified and standard airfoils. However, the drag coefficient value is higher than the standard. The greatest torque was discovered in blade code 4T-4LT (4412 TE mod-4412 LE-TE mod), which is affected by the lift and drag coefficients. Designing a high torque HAWT rotor must consider the lift and drag coefficient values.

The rotational speed of the wind turbine influences TSR. The higher the TSR, the greater the angular velocity, which enhances the wind turbine's power and power coefficient. The maximum TSR was generated in the 4LT-2LT blade code, which results in the highest HAWT power and power coefficient. Blade designs of the C4412-2412 group combination, especially blade codes 4L-2LT, 4T-2LT, 4LT-2L, 4LT-2T, and 4LT-2LT, can produce more than 1MW. High torque does not always equate to high power values; instead, the TSR value as a function of angular speed influences this. The aerodynamics of the rotor blade obviously affect the angular speed of a horizontal axis wind turbine.

Acknowledgement

This research was funded by a grant with the Basic Research scheme of the Faculty of Engineering, Universitas Negeri Semarang in 2023.

References

[1] Sher, Farooq, Oliver Curnick, and Mohammad Tazli Azizan. "Sustainable conversion of renewable energy sources." *Sustainability* 13, no. 5 (2021): 2940. https://doi.org/10.3390/su13052940

[2] Dallatu Abbas, U., S. K. Tiong, Ammar Ahmed Alkahtani, C. P. Chen, Gamal Alkawsi, and Janaka Ekanayake. "Power Curve Evaluation of Micro-Scale Turbines for Harvesting Wind Energy in Malaysia." *Applied Mathematics & Information Sciences an International Journal* 15, no. 1 (2021): 59-71. https://doi.org/10.18576/amis/150108

[3] Soeripno, M. S., and Nila Murti. "Wind hybrid power generation marketing development initiatives (WHyPGen)." *Respects Magazine* 3 (2013): 22-25.

[4] Scott, John. "The beaufort wind scale." *Force Land Water* (2005).

[5] Purwanto, Widodo Wahyu, Y. S. Nugroho, R. Dalimi, A. H. Soepardjo, A. Wahid, D. Supramono, D. Herminna, and T. A. Adilina. "Indonesia energy outlook and statistics." *Pengkajian Energi Universitas Indonesia, Jakarta* (2006).

[6] Tenghiri, L., Y. Khalil, F. Abdi, and A. Bentamy. "Optimum design of a small wind turbine blade for maximum power production." In *IOP Conference Series: Earth and Environmental Science*, vol. 161, no. 1, p. 012008. IOP Publishing, 2018. https://doi.org/10.1088/1755-1315/161/1/012008

[7] Wardhana, Agum Try, Ahmad Taqwa, and Tresna Dewi. "Design of Mini Horizontal Wind Turbine for Low Wind Speed Area." In *Journal of Physics: Conference Series*, vol. 1167, no. 1, p. 012022. IOP Publishing, 2019. https://doi.org/10.1088/1742-6596/1167/1/012022

[8] Kriswanto, Kriswanto, Muhammad Adnan Bayu Setiawan, Dony Hidayat Al-Janan, Rizqi Fitri Naryanto, Ahmad Roziqin, Hendrix Noviyanto Firmansyah, Rizki Setiadi, Febri Budi Darsono, Andri Setiyawan, and Jamari Jamari. "Power Optimization of The Horizontal Axis Wind Turbine Capacity of 1 MW on Various Parameters of The Airfoil, an Angle of Attack, and a Pitch Angle." *Journal of Advanced Research in Fluid Mechanics and Thermal Sciences* 103, no. 2 (2023): 141-156. https://doi.org/10.37934/arfmts.103.2.141156

[9] Mujahid, Muhammad, Abdur Rafai, Muhammad Imran, Mustansar Hayat Saggu, and Noor Rahman. "Design optimization and analysis of rotor blade for horizontal-axis wind turbine using Q-blade software." *Pakistan Journal of Scientific & Industrial Research Series A: Physical Sciences* 64, no. 1 (2021): 65-75. https://doi.org/10.52763/PJSIR.PHYS.SCI.64.1.2021.65.75

[10] Muhsen, Hani, Wael Al-Kouz, and Waqar Khan. "Small wind turbine blade design and optimization." *Symmetry* 12, no. 1 (2019): 18. https://doi.org/10.3390/sym12010018

[11] Oukassou, Karim, Sanaa El Mouhsine, Abdellah El Hajjaji, and Bousselham Kharbouch. "Comparison of the power, lift and drag coefficients of wind turbine blade from aerodynamics characteristics of Naca0012 and Naca2412."

Procedia Manufacturing 32 (2019): 983-990. https://doi.org/10.1016/j.promfg.2019.02.312
[12] Rocha, P. A. Costa, J. W. Carneiro de Araujo, R. J. Pontes Lima, M. E. Vieira da Silva, D. Albiero, C. F. de Andrade, and F. O. M. Carneiro. "The effects of blade pitch angle on the performance of small-scale wind turbine in urban environments." *Energy* 148 (2018): 169-178. https://doi.org/10.1016/j.energy.2018.01.096
[13] Suresh, A., and S. Rajakumar. "Design of small horizontal axis wind turbine for low wind speed rural applications." *Materials Today: Proceedings* 23 (2020): 16-22. https://doi.org/10.1016/j.matpr.2019.06.008
[14] Zahariea, D., D. E. Husaru, and C. M. Husaru. "Aerodynamic and structural analysis of a small-scale horizontal axis wind turbine using QBlade." In *IOP Conference Series: Materials Science and Engineering*, vol. 595, no. 1, p. 012042. IOP Publishing, 2019. https://doi.org/10.1088/1757-899X/595/1/012042
[15] Kunya, Bashir Isyaku, Clement O. Folayan, Gyang Yakubu Pam, Fatai Olukayode Anafi, and Nura Muaz Muhammad. "Experimental and Numerical Study of the Effect of Varying Sinusoidal Bumps Height at the Leading Edge of the NASA LS (1)-0413 Airfoil at Low Reynolds Number." *CFD Letters* 11, no. 3 (2019): 129-144.
[16] Kriswanto, Kriswanto, Fajar Romadlon, Dony Hidayat Al-Janan, Widya Aryadi, Rizqi Fitri Naryanto, Samsudin Anis, Imam Sukoco, and Jamari Jamari. "Rotor Power Optimization of Horizontal Axis Wind Turbine from Variations in Airfoil Shape, Angle of Attack, and Wind Speed." *Journal of Advanced Research in Fluid Mechanics and Thermal Sciences* 94, no. 1 (2022): 138-151. https://doi.org/10.37934/arfmts.94.1.138151
[17] Radhakrishnan, Jayakrishnan, and Dhruv Suri. "Design and optimisation of a low reynolds number airfoil for small horizontal axis wind turbines." In *IOP Conference Series: Materials Science and Engineering*, vol. 377, no. 1, p. 012053. IOP Publishing, 2018. https://doi.org/10.1088/1757-899X/377/1/012053
[18] Altmimi, Amani I., Aya Aws, Muhsin J. Jweeg, Azher M. Abed, and Oday I. Abdullah. "An investigation of design and simulation of horizontal axis wind turbine using QBlade." *Measurement Science Review* 22, no. 6 (2022): 253-260. https://doi.org/10.2478/msr-2022-0032
[19] Akbari, Vahid, Mohammad Naghashzadegan, Ramin Kouhikamali, Farhad Afsharpanah, and Wahiba Yaïci. "Multi-objective optimization and optimal airfoil blade selection for a small horizontal-axis wind turbine (HAWT) for application in regions with various wind potential." *Machines* 10, no. 8 (2022): 687. https://doi.org/10.3390/machines10080687
[20] Samosir, Ahmad Saudi, and A. Riszal. "The effect analysis of wind speed variation to the horizontal axis wind turbine design with Q-blade." In *IOP Conference Series: Materials Science and Engineering*, vol. 1173, no. 1, p. 012009. IOP Publishing, 2021. https://doi.org/10.1088/1757-899X/1173/1/012009
[21] Kunya, Bashir Isyaku, Clement Olaloye Folayan, Gyang Yakubu Pam, Fatai Olukayode Anafi, and Nura Mu'az Muhammad. "Performance study of whale-inspired wind turbine blade at low wind speed using numerical method." *CFD Letters* 11, no. 7 (2019): 11-25.
[22] Hakim, Muhammad Syahmi Abdul, Mastura Ab Wahid, Norazila Othman, Shabudin Mat, Shuhaimi Mansor, Md Nizam Dahalan, and Wan Khairuddin Wan Ali. "The effects of Reynolds number on flow separation of Naca Aerofoil." *Journal of Advanced Research in Fluid Mechanics and Thermal Sciences* 47, no. 1 (2018): 56-68.
[23] Ali, Jaffar Syed Mohamed, and M. Mubin Saleh. "Experimental and Numerical Study on the Aerodynamics and Stability Characteristics of a Canard Aircraft." *Journal of Advanced Research in Fluid Mechanics and Thermal Sciences* 53, no. 2 (2019): 165-174.
[24] Tajuddin, Nurulhuda, Shabudin Mat, Mazuriah Said, and Shumaimi Mansor. "Flow characteristic of blunt-edged delta wing at high angle of attack." *Journal of Advanced Research in Fluid Mechanics and Thermal Sciences* 39, no. 1 (2017): 17-25.
[25] Brella, Rohan, Mayank Sehgal, and Naveen Kumar. *Design and Optimization of Composite Horizontal Axis Wind Turbine (Hawt) Blade*. No. 2018-01-1034. SAE Technical Paper, 2018. https://doi.org/10.4271/2018-01-1034
[26] Hachim, Ghanim M., and Jaafar A. Mahdi. "Analytical Assessment of the Effects of Blade Cone Angle on the Aerodynamic Performance of the Horizontal Axis Wind Turbine." In *IOP Conference Series: Materials Science and Engineering*, vol. 671, no. 1, p. 012140. IOP Publishing, 2020. https://doi.org/10.1088/1757-899X/671/1/012140
[27] Umar, Dallatu Abbas, Chong Tak Yaw, Siaw Paw Koh, Sieh Kiong Tiong, Ammar Ahmed Alkahtani, and Talal Yusaf. "Design and optimization of a small-scale horizontal axis wind turbine blade for energy harvesting at low wind profile areas." *Energies* 15, no. 9 (2022): 3033. https://doi.org/10.3390/en15093033
[28] Mahmuddin, Faisal. "Rotor blade performance analysis with blade element momentum theory." *Energy Procedia* 105 (2017): 1123-1129. https://doi.org/10.1016/j.egypro.2017.03.477
[29] Moriarty, Patrick J., and A. Craig Hansen. *AeroDyn theory manual*. No. NREL/TP-500-36881. National Renewable Energy Lab., Golden, CO (US), 2005. https://doi.org/10.2172/15014831
[30] Gray, Abhishek, Bhupinder Singh, and Supreet Singh. "Low wind speed airfoil design for horizontal axis wind turbine." *Materials Today: Proceedings* 45 (2021): 3000-3004. https://doi.org/10.1016/j.matpr.2020.11.999
[31] Bourhis, Martin, Michaël Pereira, Florent Ravelet, and Ivan Dobrev. "Innovative design method and experimental investigation of a small-scale and very low tip-speed ratio wind turbine." *Experimental Thermal and Fluid Science*

130 (2022): 110504. https://doi.org/10.1016/j.expthermflusci.2021.110504
[32] Siemens. "SG 2.1-114 Onshore wind turbine." *Siemens Gamesa Renewable Energy*. Accessed September 19, 2023. https://www.siemensgamesa.com/products-and-services/onshore/wind-turbine-sg-2-1-114.
[33] Yin, Rui, Jian-Bin Xie, and Ji Yao. "Optimal Design and Aerodynamic Performance Prediction of a Horizontal Axis Small-Scale Wind Turbine." *Mathematical Problems in Engineering* 2022, no. 1 (2022): 3947164. https://doi.org/10.1155/2022/3947164
[34] Koç, Emre, Onur Günel, and Tahir Yavuz. "Comparison of Qblade and CFD results for small-scaled horizontal axis wind turbine analysis." In *2016 IEEE International Conference on Renewable Energy Research and Applications (ICRERA)*, pp. 204-209. IEEE, 2016. https://doi.org/10.1109/ICRERA.2016.7884538
[35] Takey, Mohamed, Tholudin Mat Lazim, Iskandar Shah Ishak, N. A. R. Nik Mohd, and Norazila Othman. "Computational Investigation of a Wind Turbine Shrouded with a Circular Ring." *CFD Letters* 12, no. 10 (2020): 40-51. https://doi.org/10.37934/cfdl.12.10.4051
[36] Zakaria, Ahmad, and Mohd Shahrul Nizam Ibrahim. "Velocity Pattern Analysis of Multiple Savonius Wind Turbines Arrays." *CFD Letters* 12, no. 3 (2020): 31-38. https://doi.org/10.37934/cfdl.12.3.3138
[37] Ledoux, Jeremy, Sebastián Riffo, and Julien Salomon. "Analysis of the blade element momentum theory." *SIAM Journal on Applied Mathematics* 81, no. 6 (2021): 2596-2621. https://doi.org/10.1137/20M133542X
[38] Velázquez, Miguel Toledo, Marcelino Vega Del Carmen, Juan Abugaber Francis, Luis A. Moreno Pacheco, and Guilibaldo Tolentino Eslava. "Design and experimentation of a 1 MW horizontal axis wind turbine." *Journal of Power and Energy Engineering* 2014 (2014). https://doi.org/10.4236/jpee.2014.21002
[39] Marten, David, Jan Wendler, Georgios Pechlivanoglou, Christian Navid Nayeri, and Christian Oliver Paschereit. "QBLADE: an open source tool for design and simulation of horizontal and vertical axis wind turbines." *International Journal of Emerging Technology and Advanced Engineering* 3, no. 3 (2013): 264-269.
[40] Koç, Emre, Onur Gunel, and Tahir Yavuz. "Mini-Scaled Horizontal Axis Wind Turbine Analysis By Qblade And CFD." *International Journal of Energy Applications and Technologies* 3, no. 2 (2016): 87-92.
[41] Marten, David, Matthew Lennie, Georgios Pechlivanoglou, Christian Navid Nayeri, and Christian Oliver Paschereit. "Implementation, optimization and validation of a nonlinear lifting line free vortex wake module within the wind turbine simulation code QBlade." In *Turbo Expo: Power for Land, Sea, and Air*, vol. 56802, p. V009T46A019. American Society of Mechanical Engineers, 2015. https://doi.org/10.1115/GT2015-43265
[42] Wendler, Juliane, David Marten, George Pechlivanoglou, Christian Navid Nayeri, and Christian Oliver Paschereit. "An unsteady aerodynamics model for lifting line free vortex wake simulations of hawt and vawt in qblade." In *Turbo Expo: Power for Land, Sea, and Air*, vol. 49873, p. V009T46A011. American Society of Mechanical Engineers, 2016. https://doi.org/10.1115/GT2016-57184
[43] Husaru, D. E., P. D. Bârsănescu, and D. Zahariea. "Effect of yaw angle on the global performances of Horizontal Axis Wind Turbine-QBlade simulation." In *IOP Conference Series: Materials Science and Engineering*, vol. 595, no. 1, p. 012047. IOP Publishing, 2019. https://doi.org/10.1088/1757-899X/595/1/012047
[44] Timmer, W. A., and C. Bak. "Aerodynamic characteristics of wind turbine blade airfoils." In *Advances in Wind Turbine Blade Design and Materials*, pp. 109-149. Woodhead Publishing, 2013. https://doi.org/10.1533/9780857097286.1.109
[45] Pourrajabian, Abolfazl, Maziar Dehghan, and Saeed Rahgozar. "Genetic algorithms for the design and optimization of horizontal axis wind turbine (HAWT) blades: A continuous approach or a binary one?." *Sustainable Energy Technologies and Assessments* 44 (2021): 101022. https://doi.org/10.1016/j.seta.2021.101022
[46] Kim, Youjin, Galih Bangga, and Antonio Delgado. "Investigations of HAWT Airfoil Shape Characteristics and 3D Rotational Augmentation Sensitivity Toward the Aerodynamic Performance Improvement." *Sustainability* 12, no. 18 (2020): 7597. https://doi.org/10.3390/su12187597